**Babeș - Bolyai University**
**Faculty of Chemistry and Chemical Engineering**
**Chemistry PhD School**

---

# Nanocomposite coatings for anticorrosion protection of some metals

---

**PhD Thesis Summary**

*Joury President:*

**D-na Prof. Dr. Luminiţa SILAGHI-DUMITRESCU**, Universitatea Babeş-Bolyai, Cluj Napoca

*Referees:*

**Dl. Prof. Dr. Aurel POP,** Facultatea de Fizică, Universitatea Babeş-Bolyai, Cluj Napoca

**Dl. Prof. Dr. Nicolae VASZILCSIN,** Universitatea Politehnică Timişoara

**Dl. Conf. Dr. Horaţiu VERMEŞAN,** Universitatea Tehnică Cluj-Napoca

*Scientific Advisor:*

**D-na Prof. Dr. Liana MUREŞAN,** Universitatea Babeş-Bolyai, Cluj Napoca

**Public defense: 13 Decembrie 2013**

# PhD Thesis Table Of Contents

Acknowledgements 2

Introduction 7

**CHAPTER I. THEORETICAL ASPECTS**

1. Metal-nanoparticles composite coatings 10
    - 1.1 Types of particles 10
    - 1.2 Types of composite coatings 13
        - 1.2.1 Coatings with enhanced mechanical properties 13
        - 1.2.2 Self-lubricating coatings 14
        - 1.2.3 Corrosion-resistant coatings 14
    - 1.3 Electrolytical codeposition 15
        - 1.3.1 Codeposition mechanism 15
2. Zinc electrodeposition 22
    - 2.1 General aspects 22
    - 2.2 Plating baths used in zinc electrodeposition 24
        - 2.2.1 Alcaline electrolytes 24
        - 2.2.2 Neutral electrolytes 24
        - 2.2.3 Acid electrolytes 25
            - 2.2.3.1 Sulphate-based electrolytes 25
            - 2.2.3.2 Chloride-based electrolytes 27
            - 2.2.3.3 Fluoroborate-based electrolytes 29
    - 2.3 Determining parameters of electrodeposition for the properties of nanocomposite coatings 31
        - 2.3.1 Electrolyte composition 31
        - 2.3.2 Type of particles 32
        - 2.3.3 Particle concentration in the electrolyte 32
        - 2.3.4 Current density 32
        - 2.3.5 Stirring 32
3. Zinc-nanoparticle coatings 35
    - 3.1 General aspects 35

3.2 Properties 36
4. Analytical methods 36
4.1. Electrochemical methods 36
4.1.1 Open-circuit potential 36
4.1.2 Polarization curves 36
4.1.3 Electrochemical impedance spectroscopy 38
4.2. Morpho-structural characterizations 39
4.2.1 AFM 39
4.2.2 SEM 41
4.2.3 EDXS 43
4.2.4 X-ray diffraction 44
4.2.5 GDOES 45

**CHAPTER II. ORIGINAL CONTRIBUTIONS**

5. Introduction 47
6. Influence of the electrodeposition current regime on the corrosion resistance of Zn-$CeO_2$ nanocomposite coatings 48
6.1 General aspects 48
6.2 Experimental section 49
6.3 Results and discussion
6.3.1 Determination of the optimal experimental parameters 53
6.3.2 Morphological and structural investigations of the coatings 59
6.3.2.1 SEM and EDX analysis 59
6.3.2.2 Zn-$CeO_2$ coatings depth-profile 61
6.3.2.3 Microhardness 68
6.3.3 Corrosion measurements 69
6.4 Conclusions 72
7. Initial corrosion behavior of composite coatings obtained by co-electrodeposition of zinc with nanoparticles of Ti and Ce oxides 74
7.1 General aspects 74
7.2 Experimental section 75
7.2.1 Materials 75
7.2.2. Methods 76

- 7.3. Results and discussions 80
  - 7.3.1 Electrochemical measurements 80
    - 7.3.1.1 Open-circuit potential 80
    - 7.3.1.2 Potentiodynamic measurements 81
    - 7.3.1.3 Electrochemical impedance spectroscopy 84
  - 7.4.1 Morpho-structural characterizations 89
    - 7.4.1.1 AFM 89
    - 7.4.1.2 X-ray diffraction 91
    - 7.4.1.3 SEM and EDX analysis 91
    - 7.4.1.4 Salt spray tests 93
- 7.5 Conclusions 97

8. Corrosion behaviour of composite coatings with nanoparticles of $CeO_2$ $ZrO_2$ binary oxides 98
- 8.1 General aspects 98
- 8.2 Experimental section 99
  - 8.2.1 Materials 99
  - 8.2.2 Methods 99
- 8.3 Results and discussions 101
  - 8.3.1 Morpho-structural analysis 101
    - 8.3.1.1. SEM and EDX analysis 101
    - 8.3.1.2 X-ray diffraction 103
  - 8.3.2 Electrochemical measurements 104
    - 8.3.2.1 Open circuit potential 104
    - 8.3.2.2 Potentiodynamic measurements 104
- 8.4 Conclusions 108

9. General conclusions 109

10. Perspectives 111

11. References 111

12. Publications and scientific proceedings list 124

## KEYWORDS

Electrodeposition, nanoparticles, pulsed current, direct current, binary oxides, $CeO_2$, $TiO_2$, $ZrO_2$, corrosion, nanocomposite coatings, GDOES, SEM, EDX, saline fog, electrochemical measurements, potentiodynamic curves

## ABBREVIATIONS

SEM – Scanning electron microscopy

GDOES – Glow-discharge optical emission spectroscopy

EDX – Energy dispersion X-ray spectroscopy

EIS – Spectroscopie electrochimică de impedanţă

$i_{corr}$ – corrosion current density

$E_{corr}$ – corrosion potential

# Introduction

In the last decades there was a need to improve the corrosion resistance of steel-based materials, used commonly in all industries. This fact has promoted various treatment methods, the most efficient being the electrochemical methods. Using these techniques the obtained coating or composite materials consisting of metals can have enhanced corrosion properties. These methods offer unique opportunities and significant advantages in the development of new materials: rigorous control of the deposited layers' thickness can be made easily, the quickness of deposition of materials can be easily controlled by adjusting the electrodeposition parameters, the required temperature is relatively low (room temperature), the equipment is relatively affordable and the final costs of obtaining materials can be considerably reduced.

Taking these facts into account, after a careful sweep of the literature data referring to the composite plating a series of oxide-based nanoparticles has appeared, which have been used as dopants for the metal composite coatings with promising results. Composite-based deposits were obtained using ZnO, $Al_2O_3$, $ZrO_2$, $TiO_2$, $WS_2$, $MoS_2$, $CeO_2$, $CeO_2$·and $TiO_2$ with a variety of metals and alloys in order to create materials with superior properties [1-7, 25]. Among the obtaining methods of these materials one of the most efficient ones were the pulsed current and the reversed pulsed current electrodeposition [8-10]. Their use to obtain composite materials has led to significant changes in the quality of deposits, altering the structural, morphological and electrochemical characteristics. Among the improved properties it has to be mentioned the microhardness, corrosion resistance, low friction coefficients and the resistance to higher loads.

In this context, the objectives of the original part of the thesis are focused on the:

- investigation of the possibilities of obtaining composite coatings based on Zn and $CeO_2$ nanoparticles using electrodeposition in both pulsed and direct current and comparison of their properties (such as microstructure, morphology, microhardness and corrosion resistance) with those of pure zinc coatings, obtained in the same experimental conditions;
- obtaining and characterization of composite coatings Zn-Ti and Ce based oxide nanoparticles, where the oxides were used separately, in mixture and in the form of binary oxides in order to correlate the properties of the nanoparticles with the obtained composite coatings;

- obtaining and characterization of Zn-$CeO_2$•$ZrO_2$ nanoparticles and the comparison with coatings made using a mechanical mixture of $CeO_2$ and $ZrO_2$.

The thesis is divided into two main sections. The first part presents the theoretical aspects related to metallic coatings, based on an overview of the current state of the art, continued with the most important aspects of Zn-based composite coatings, their properties and analytical methods used for their characterization. The second part is dedicated to original contributions, which are divided into three main sections:

- in the first chapter, *Influence of the electrodeposition current regime on the corrosion resistance of Zn-$CeO_2$ nanocomposite coatings* the aim was to determine an optimal concentration of $CeO_2$ nanoparticles in coatings by morpho-structural methods, following by a presentation and discussion of results related to changes of the current regime used, continuous and pulsed current and the way how this affects the morphology of the surface and the corrosion resistance of these metallic coatings;
- the second chapter discusses the *Initial corrosion behavior of composite coatings obtained by co-electrodeposition of Zn with nanoparticles of Ti and Ce oxides*. In this section a comparison is made between simple composite coatings only with $TiO_2$ or $CeO_2$, binary oxides of these oxides and mixture of simple oxides, obtained by mechanical combination. The electrochemical properties of metallic coatings were obtained by specific tests and the morphology of the surface was determined using various morphostructural methods, determining the effects of the presence of the binary nanoparticles, mixed or simple in the composite zinc coatings.

the third chapter continues the investigation of the binary oxides, focusing on the Corrosion behaviour of composite coatings with nanoparticles of *$CeO_2$·$ZrO_2$ binary oxides*. In this part, the effects of incorporation of the two oxides in the Zn coatings in terms of electrochemical and morpho-structural characterization are presented and discussed, followed by an optimization of concentration in the electrolyte, maintaining their good anti-corrosive properties.

# CHAPTER II. ORIGINAL CONTRIBUTIONS

## Introduction

After a state of the art sweep, referring to composite metallic coatings, several types of nanoparticles with interesting properties have been selected and used to obtain nanocomposite coatings with enhanced anticorrosion properties.

Among the modified properties of the coatings, enhanced microhardness, corrosion resistance, lower friction coefficients, higher load resistance and surfaces with a lower granulation stand out.

Within this context, the objectives of the original research of this thesis are:

- The investigation of the possibility of obtaining Zn-$CeO_2$ nanocomposite coatings by using pulsed and direct-current electrodeposition at different frequencies, followed by a morpho-structural investigation and a comparison of the coatings' properties versus the pure Zn reference deposit.
- Obtaining and characterization of composite Zn-nanoparticle coatings with Ti and Ce oxides, in which the nanoparticles used were binary, as a mixture of separate oxides and simple oxides, in an attempt to correlate properties of nanoparticles with the characteristics of the obtained coatings.
- The preparation and characterization of Zn-nanoparticles coatings with $CeO_2 \cdot ZrO_2$ binary oxides, the separate simple oxides and the mechanical mixture between $CeO_2$ and $ZrO_2$, in an attempt to compare the anti-corrosion properties of the obtained deposits.

In order to achieve these objectives, different experimental methods have been employed, both electrochemical (galvanostatic electrodeposition, open circuit potential measurements, liniar polarization, etc) and morpho-structural methods (SEM, XRD, GDOES, etc)

# 6. Influence of the electrodeposition current regime on the corrosion resistance of Zn-$CeO_2$ nanocomposite coatings

## 6.1 General aspects

Cerium oxide possesses some interesting characteristics which recommend it for applications in various fields. The antioxidant and thermal barrier properties of nano ceria have been previously reported by Ivanov *et al.* [98] and Cao *et al.* [99]. The barrier properties are due to the lower thermal diffusivity and higher thermal expansion coefficient of $CeO_2$ than those of other oxides (*e.g.* $ZrO_2$). Other common applications of ceria are in construction of fuel cells, manufacture of sensors, in catalysis etc. [1]. On the other hand, cerium compounds, used either as coatings [100] or as inhibitors [101-103] are known to hinder the cathodic reactions, thereby inhibiting corrosion [104, 105]. Therefore, cerium oxide particles have been used to obtain composite coatings with various metals such as zinc, nickel etc. Incorporation of $CeO_2$ nanoparticles in the metallic matrix can significantly improve the materials properties, such as wear, corrosion and temperature oxidation resistance, microhardness etc. In the case of zinc coatings, it was proven that the embedded nanoparticles contribute to lowering of the alloying reaction between zinc and iron, and enhance the barrier protection of the interior layers of zinc coatings [104]. Moreover, embedded $CeO_2$ nanoparticles can diminish the grain size of metallic deposits obtained by electrodeposition by stimulating nucleation [2,8,105-110].

Shibli and Chacko [104] have studied the properties of Zn–$CeO_2$ obtained by a hot–dip process. They noticed an improved corrosion resistance of the zinc layers upon addition of ceria. S. Ranganatha *et al.* [1] confirmed also that the addition of $CeO_2$ improved the anticorrosion properties of the zinc deposits obtained by using electrodeposition.

Electrodeposition is one of the most cost–effective and efficient methods of obtaining composite zinc coatings, which grants the possibility of controlling the deposit’s thickness, the current regime, potential, and room temperature working conditions. It was reported that composites of desired properties may be prepared by using an adequate choice of the electrodeposition parameters and of the particle concentration in the plating electrolytes. It has also been showed that the particle size has a significant influence on the final properties of the composite coating [13]

There has been a number of research works on zinc that have reported the successful obtaining of composite coatings *via* direct current [1,16,19,111,112], pulsed current [8,9,48,113] or reversed pulse current [10,115]. It has been shown that the use of pulsed current may ensure finer granulation of the deposit [113], thus a better corrosion resistance of a galvanostatically obtained deposit.

In order to gain deeper insight on the relationship existing between the type of applied current and the properties of Zn–$CeO_2$ composites prepared by electrodeposition, the present work investigated the influence of the current regime on the microstructure, microhardness, content profile and the corrosion parameters of Zn–$CeO_2$ deposits, in comparison with those of pure zinc samples obtained under identical experimental conditions.

## 6.3 Results and discussions

### 6.3.1. Determination of the optimal experimental parameters

In order to obtain composite deposits with enhanced properties, the optimal plating parameters have been determined from SEM micrographs and GDOES analysis. For the electrodeposition cell, in order to visualize the presence and influence of the nanoparticles in the deposit, the electrolyte without additives has been put to use.

Thus, zinc deposits have been obtained, from a chloride-based electrolyte, with a known composition, in which two types of brightening agents have been added in turns, agents commonly used in industrial plating baths (ZetaPlus – brightening agents).

After considering the results from the morphologic analysis of the obtained deposits at 1 $A/dm^2$ respectively at 2 $A/dm^2$, from the additive-free electrolyte (Fig. 6.6-thesis), it has been determined that the 2 $A/dm^2$ deposits are more compact than the others, being prone to having a higher corrosion resistance, due to the fact that less corrosion sites are present on the surface. Also, considering the effects of the nanoparticles on the surface at 5,10 and 20 g/L, in correlation with the GDOES analysis, the 20 g/L concentration has been chosen, due to the fact that the concentration in the deposit is higher, and that the surface modifications are much clearer.

Thus, these are the parameters that have been chosen to further continue the research.

### 6.3.2 Morphological and structural investigations of the coatings

#### 6.3.2.1. SEM and EDX analysis

The morpho-structural study of the composite coatings was done with the help of a scanning electron microscope (SEM). The representative micrographs of the surfaces and cross-sections are presented in Fig. 6.11-6.14.

The pure zinc deposits obtained in direct current (Fig. 6.11-a), present a rough surface, with very compact, small hexagonal platelets. This arrangement is similar to that observed in the case of zinc electrodeposits prepared from sulphate–based electrolytes in the absence of any additive [61].

The change of current regime to pulsed current seems to have a beneficial effect on the grain refinement, creating smoother surfaces and increasing the compactness of the deposit (Fig. 6.11b–e). The frequency of the pulsed current influences only slightly the deposit morphology, mainly by changing its grain size. Because the deposits obtained with pulsed current are more compact, uniform and grain–refined (Fig. 6.11b–6.11e) than those prepared with DC current, they could be candidates for better corrosion resistant coatings.

The cross section examination of the sample obtained in direct current (Fig. 6.12-a) put on evidence a relatively random orientation of the crystals in the deposit. The coating fully covers the steel substrate with rather coarse grains. This aspect slightly changed when PC regime was used. Thus, a grain refinement together with an increase of the deposit compactness and the appearance of columnar growth are noticed, especially at higher frequencies of the pulsed current (Figs. 6.12-b–e). The fact that the grain size, texture and porosity of the deposits are affected during pulse plating was already reported in the literature [70].

The addition of $CeO_2$ in the plating bath positively affected the morphology of the deposited composite coatings, leading to grain refinement, most probably through the modification of the competition between nucleation and crystal growth [1]. The co–deposition process is a competition between the $Zn^{2+}$ ions and the oxide particles for the active sites of the surface. The adsorption or incorporation of these particles at the active growth sites of a crystal will inhibit its growth, and consequently finer grained structure will be obtained [115]. In comparison to the pure zinc coating obtained by direct current (Fig. 6.11-a), the composite Zn–$CeO_2$ deposit obtained in the same current regime is much more compact, the hexagonal plates are smaller and much more coherently arranged (Fig. 6.13-a).

The use of pulsed current instead of a direct current regime in the case of Zn–$CeO_2$ nanocomposite deposits seems to further reduce the grain size in comparison both to the pure zinc sample and the composite sample obtained in DC regime (Fig. 6.13-b–e). Moreover, a close examination of the cross sections of the composite samples revealed a clearer laminar columnar growth (Fig. 6.14). The grains are arranged in a more compact manner, offering a flatter surface, leaving little room for corrosion starting points (Fig. 6.14-b–c). The insets in Fig. 6.12-a-e indicate the presence of the $CeO_2$ particles on the top of zinc platelets. The presence of nano–sized $CeO_2$ particles in the zinc deposits was confirmed by SEM – EDX analysis. Fig. 6.15 depicts a Zn–$CeO_2$ sample, obtained *via* direct current, in cross–section. The EDX analysis demonstrates the presence of Ce and O in the analyzed area, indicating a presence of $CeO_2$ nanoparticles inside the metallic deposit.

### 6.3.2.2 Zn-$CeO_2$ coatings depth-profile

In order to evaluate the $CeO_2$ repartition in the depth of the composite films, GDOES profiles of the samples were recorded and one representative result is depicted in Fig.6.16 (PhD Thesis).

$CeO_2$ was detected in the coatings, the highest incorporation degree of particles occurring when direct current was used, followed by the cases of 10 Hz and 0.1 Hz pulsed current. The Ce content in the coatings calculated as the average value obtained from two separate measurements, on the same deposit varies between 0.011 and 0.034 % (w/w). (Table 6.1)

It can be noticed that cerium can be found not only on the top of the Zn surface, but also in depth of the deposit, suggesting the presence of evenly distributed ceria nanoparticles throughout the coating, even if in a rather small concentration. However, it was proven that this low incorporated amount of ceria is sufficient to induce microstructural changes, as it can be seen in Figs. 6.11–6.15.

Surprisingly, the presence of cerium ions was detected also inside the Fe substrate, probably due to a mechanical entrapment of $CeO_2$ particles in the micro defects created on steel substrate by polishing, after its immersion in the plating bath. On the other hand, the high cerium signal existent at the top of the samples can be assigned to adsorbed $CeO_2$ nanoparticles on zinc surface, which could not be discarded by simple washing.

***Table 6.1*** *Nanoparticle contents in the obtained Zn-$CeO_2$ coatings*

| **Current regime** | **Ce**<br>**% w/w** | **$CeO_2$**<br>**% w/w** |
|---|---|---|
| **DC** | 0.0335 ±0.0077 | 0.041 ±0.0095 |
| **PC 0.01 Hz** | 0.0125 ±0.005 | 0.0153 ±0.006 |
| **PC 0.1 Hz** | 0.0135 ±0.003 | 0.0165 ±0.004 |
| **PC 1 Hz** | 0.0105 ±0.003 | 0.0129 ±0.004 |
| **PC 10 Hz** | 0.0260 ±0.008 | 0.031 ±0.01 |

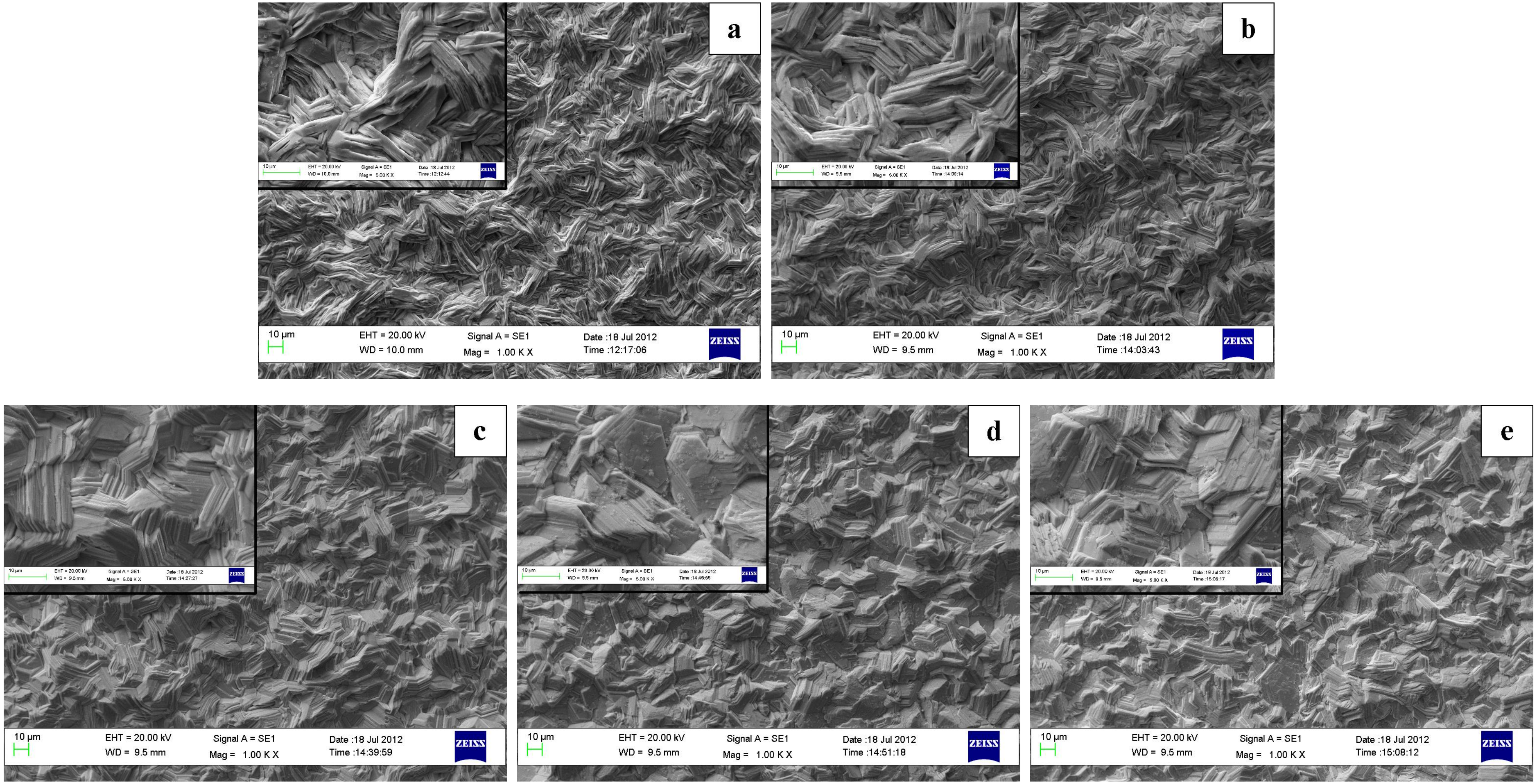

**Fig. 6.12.** SEM images of composite zinc–$CeO_2$ deposits obtained in (a) direct current, (b) PC 0.01 Hz, (c) PC 0.1 Hz, (d) PC 1 Hz, (e) PC 10 Hz

### 6.3.2.3 Microhardness

The $HV_{0.01}$ microhardness values for the investigated samples, estimated as the mean of 12 measurements per sample, varied between 38.43 and 44.67 $HV_{(0.01)}$. A comparison between the microhardness of the different samples is presented in Figure 6.16.

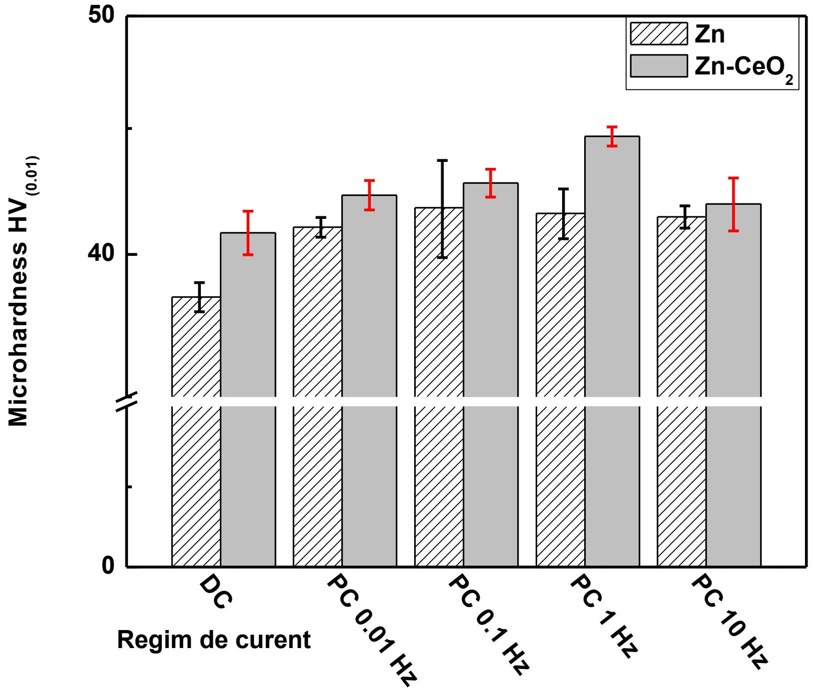

*Fig. 6.16. Rezultatele testului de microduritate (HV 0.01) pentru depunerile de zinc pur si cele compozite Zn-*$CeO_2$ *obținute utilizând diferite regimuri de curent*

For the same current regime, the addition of ceria in the zinc deposit increased its microhardness by up to 7%, not necessarily as a consequence of particles inclusion, but because of the decrease of the grain size and the increase of deposit compactness. The microhardness values were slightly higher when PC regime was used, the highest value corresponding to the nanocomposite deposits produced under PC at 1 Hz and 0.1 Hz.

### 6.3.3 Corrosion measurements

In order to determine the corrosion parameters of the obtained composite deposits, electrochemical polarization tests have been completed. Thus, both kinetical parameters and the polarization resistances of the corrosion process, respectively the coatings, have been determined for the composite deposits.

After ±25 mV *vs* OCP linear sweeps, in a $Na_2SO_4$ 7.1 g/L corrosive medium, at 20 hours immersion time, the results in Fig. 6.17 have been obtained.

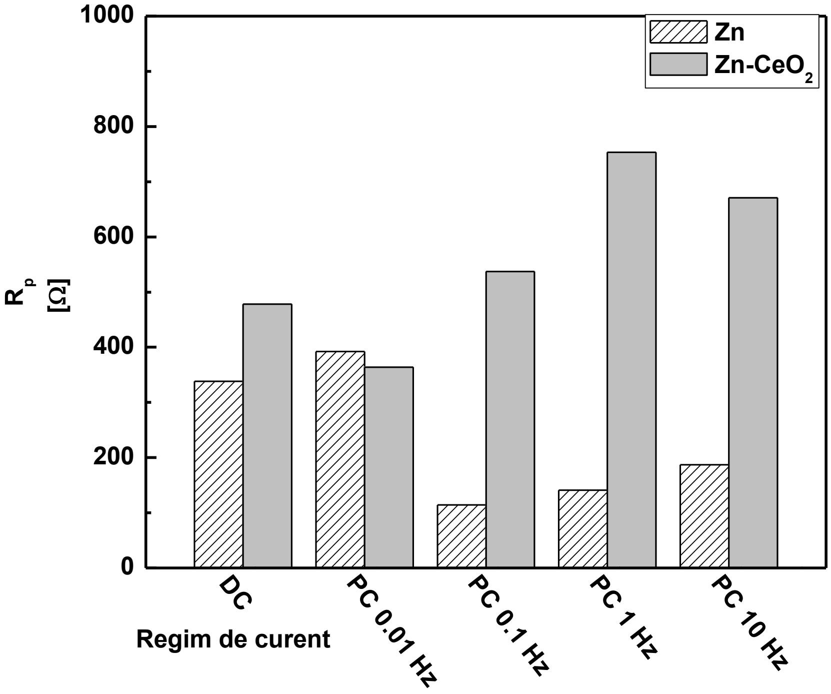

***Fig. 6.17*** *Polarization resistance data, obtained from ±25 mV vs OCP at 20 hours immersion time in* $Na_2SO_4$

***Table 6.2*** *Potentiodynamic curves interpretation results (+300 - -800 mV vs OCP) on Zn and* $Zn-CeO_2$ *deposits, obtained in direct and pulsed current*

| **Deposit** | **Current regime** | $i_{corr}$ [μA $cm^{-2}$] | $E_{corr}$ [V *vs.* Ag/AgCl] |
|---|---|---|---|
| **Zn** | DC | 4.81 | -1.15 |
| | PC 0.01 Hz | 2.12 | -1.17 |
| | PC 0.1 Hz | 1.04 | -1.31 |
| | PC 1 Hz | 0.47 | -1.21 |
| | PC 10 Hz | 2.64 | -1.15 |
| **$Zn-CeO_2$** | DC | 3.56 | -1.08 |
| | PC 0.01 Hz | 1.25 | -1.11 |
| | PC 0.1 Hz | 1.27 | -1.09 |
| | PC 1 Hz | 0.69 | -1.10 |
| | PC 10 Hz | 1.75 | -1.19 |

## 6.4 Conclusions

Zinc–$CeO_2$ deposits prepared from a chloride bath were successfully obtained on low–carbon steel substrates in direct and in pulsed current regimes. The use of pulsed current during electrodeposition leads to grain refinement and to a better compactness of the deposit.

The incorporation of nanoparticles inside the metallic matrix was clearly demonstrated by GDOES analysis of the coatings.

The presence of even minute amounts of incorporated ceria nanoparticles results in an increased microhardness and has a beneficial effect on the corrosion resistance of the zinc deposits. The addition of ceria in the plating bath renders the zinc deposit more resistant to generalized corrosion.

The study revealed that a pulsed–current regime is preferable to a direct–current approach of the electro–co–deposition process, offering more compact deposits, with better anti–corrosion properties.

# 7. Initial corrosion behavior of composite coatings obtained by co-electrodeposition of zinc with nanoparticles of Ti and Ce oxides

## 7.1. General aspects

Among the oxides used for enhancing the corrosion resistance of the coatings, $CeO_2$ and $TiO_2$ are particularly interesting, due to their resistance to high temperature oxidation, corrosion, mechanical abrasion and wear [118]. In recent years, these oxides have found new applications as dopants for silica based sol-gel corrosion protection coatings which are considered environmentally friendly by comparison with the traditional chromate conversion coatings [97,119]. $CeO_2$ incorporated in aluminum was reported as corrosion inhibitor [120], due to the fact that cerium oxides and hydroxides hinder the cathodic reduction reaction [121]. Moreover, $Ce^{4+}$ ions are able to promote the superficial oxidation of metals, conferring natural protection layer because of their high oxidation potential. Ceria layers electrodeposited from cerium nitrate solutions in the presence of PEG on zinc-electroplated steel [122] or cerium-based oxides films were elaborated by cathodic electrodeposition from relatively concentrated cerium nitrate solutions on carbon steel [123]. On the other hand, $CeO_2$ nanoparticles embedded in hot dip zinc coatings [103] caused significant improvement in galvanic and other physical characteristics of the coatings.

In what titania is concerned, it was reported that nanosized $TiO_2$ electrocodeposited with zinc confer an enhanced resistance against corrosion and better mechanical properties to the corresponding zinc coatings [16, 18, 19, 124].

Despite the number of papers reporting the beneficial effects of $CeO_2$ and $TiO_2$ on corrosion resistance of Zn coatings, to the best of our knowledge, there are no reports on the combined effect of both oxides on zinc-electroplated steel or on the use of binary $CeO_2$ $TiO_2$ oxides. Moreover, it should be mentioned that the electrolytic co-deposition of inert particles and metals is a very complex process. Although several experimental and theoretical studies on particle co-deposition mechanism have been published [66, 125-130], the process is not yet well understood.

In this context, the present work reports the results obtained for the preparation of composite Zn coatings on steel by using binary $TiO_2{\cdot}CeO_2$oxides. In an attempt to correlate the effects of nanoparticles with their characteristics and with the properties of the composite deposits, the anti-corrosion properties of Zn-$TiO_2{\cdot}CeO_2$ layers are compared with those referring to similar coatings prepared by using a simple mixture of the two oxides or the individual oxides.

## 7.3 Results and discussions

### 7.3.1 Electrochemical measurements

### 7.3.1.1 Open circuit potential

The open circuit potential values for the obtained deposits after immersion in a $Na_2SO_4$ solution (pH=5) had a gradual variation in the negative domain in the first few minutes, later being stabilized at the values shown in Table 7.2.

***Tabel 7.2***. *Valorile potențialului de circuit deschis pentru depozitele compozite*

| **Deposit** | ***OCP***<br>**[mV *vs.* Ag/AgCl$_s$]** |
|---|---|
| **Zn-$CeO_2{\cdot}TiO_2$** | -1012 |
| **Zn-$CeO_2$-$TiO_2$** | -940 |
| **Zn-$CeO_2$** | -1011 |
| **Zn-$TiO_2$** | -1001 |
| **Zn** | -983 |

### 7.3.1.2. Potentiodynamic measurements

The cathodic and anodic polarization curves for Zn and Zn−nanoparticles electrodes recorded after 1h of immersion in $Na_2SO_4$ solution (pH 5) are depicted in Figures 7.4 și 7.5.

It can be readily observed that the corrosion process in aerated $Na_2SO_4$ medium is under cathodic control (oxygen diffusion) and that the cathodic branches of the polarization curves are rather similar for all the deposits. Due to this fact, the cathodic reaction does not have a valid Tafel slope, and the corrosion current densities were determined by using the anodic slope. The corrosion parameters calculated by using the Tafel extrapolation method are given in Table 7.3.

**Tabel 7.3** Corrosion parameters estimated from the potentiodynamic measurements for the zinc and composite deposits.

| **Deposit** | $i_{corr}$ **(μA cm$^{-2}$)** | $E_{corr}$ **(mV *vs.* Ag/AgCl$_s$)** | $b_a$ **(V/dec)** | **Polarization resistance (Ω cm$^2$)** |
|---|---|---|---|---|
| **Zn−TiO$_2$·CeO$_2$** | 68.6 | −967 | 0.106 | 1552 |
| **Zn−(TiO$_2$+CeO$_2$)** | 20.2 | −950 | 0.061 | 3036 |
| **Zn−CeO$_2$** | 23.7 | −940 | 0.068 | 2865 |
| **Zn−TiO$_2$** | 39.5 | −960 | 0.073 | 1862 |
| **Zn** | 76.2 | −951 | 0.094 | 1239 |

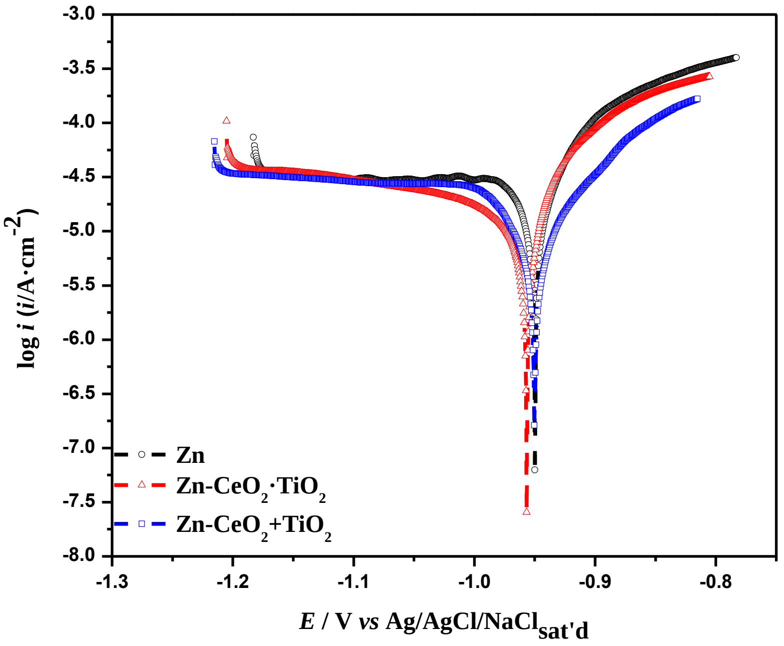

***Fig 7.4.*** *Polarization curves (±200 mV vs. OCPfor the pure Zn, Zn−TiO$_2$, and Zn−CeO$_2$ deposits*

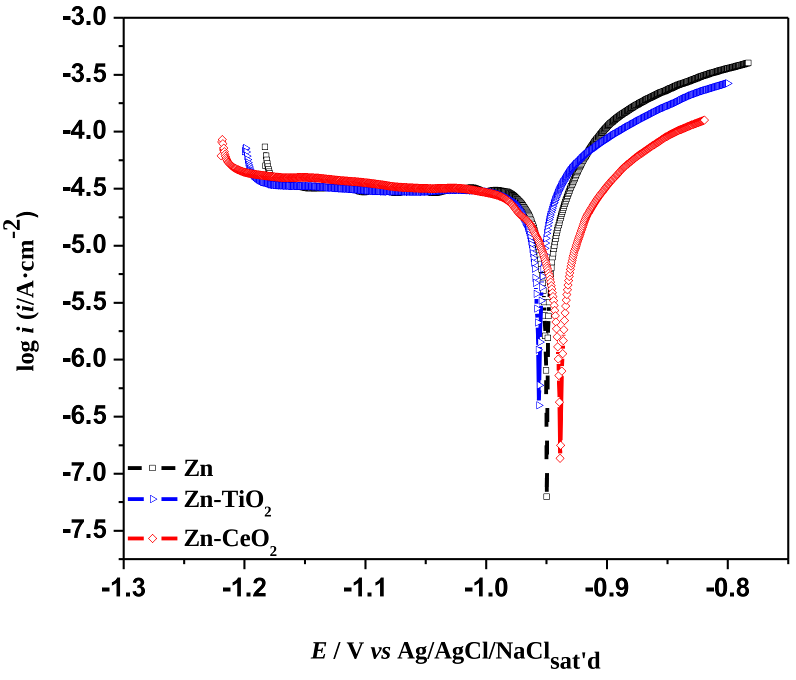

***Fig 7.5.*** *Polarization curves (±200 mV vs. OCPfor the pure Zn, Zn−$CeO_2$·$TiO_2$ and Zn−($CeO_2$+$TiO_2$)deposits*

### 7.3.1.3 Electrochemical impedance spectroscopy

In order to achieve a better understanding of the effect the incorporated nanoparticles have inside the Zn deposit, the corrosion process has been investigated through the electrochemical impedance spectroscopy method.

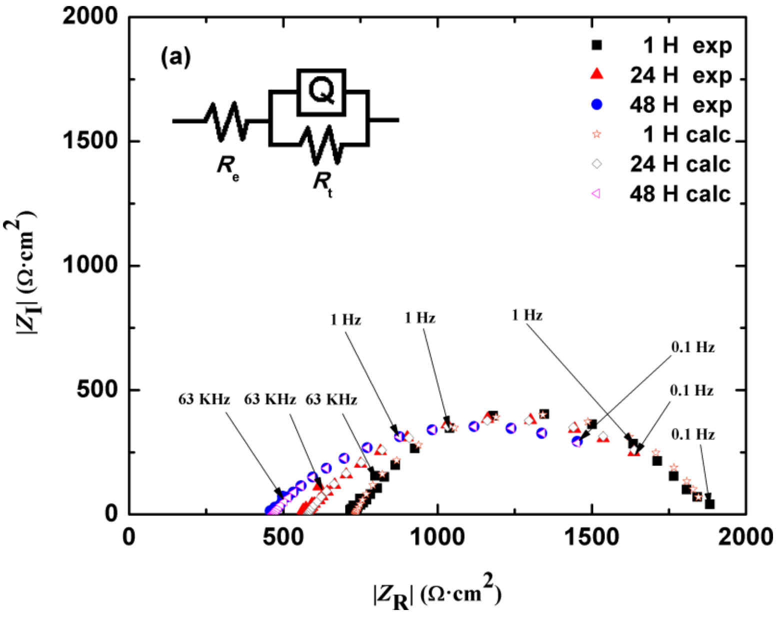

***Fig 7.7*** *Nyquist impedance diagrams of Zn−$CeO_2$·$TiO_2$ (a) and Zn (b) deposits in $Na_2SO_4$ (pH=5) solution recorded at ocp. (hollow symbols)− simulated diagrams.*

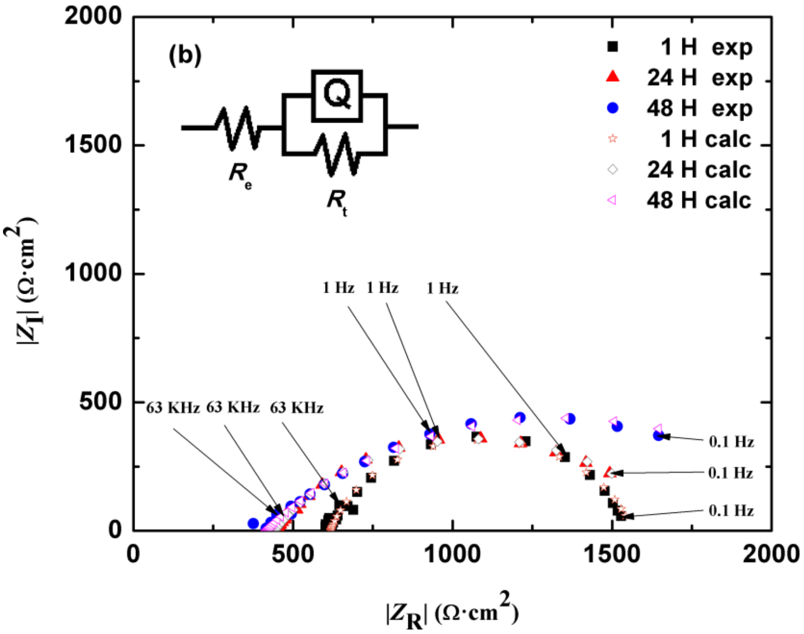

***Fig 7.7*** *Nyquist impedance diagrams of* $Zn-CeO_2{\cdot}TiO_2$ *(a) and Zn (b) deposits in* $Na_2SO_4$ *(pH=5) solution recorded at ocp. (hollow symbols)− simulated diagrams.*

The equivalent circuit used for fitting the impedance data is R(RQ). It included the electrolyte resistance, the charge transfer resistance and the double layer capacitance (Fig. 7.7 inset). For an optimal fitting, the capacitance has been changed with a constant phase element (Q), which takes into consideration both the deviation from the ideal dielectric behavior and the probable existing inhomogenities. The parallel arrangement impedance is linked with the faradaic reaction that takes place at the metal-liquid interface. The depressed capacitive loop characteristic can be described with a *n* coefficient, with values lower than 1. The lower the values, the higher the deviation of the system from an ideal capacitive behavior.

The equivalent circuit used for fitting reproduces the data with a relatively good accuracy, as it can be seen from Fig. 7.7. The full symbols from the legend are the measured data and the hollow symbols represent the fitting points.

***Table 7.4.*** *Corrosion process parameters, calculated by non-linear regression of the impedance dataset, obtained for the Zn and Zn-nanoparticles deposits.*

| **Deposit** | **Immersion time** | $R_e$ **($\Omega$ cm$^2$)** | $Q$ **(s $\Omega^{-1}$ $10^{-4}$)** | $n$ | $C_{dl}$ **($\mu$F cm$^2$)** | $R_t$ **($\Omega$ cm$^2$)** |
|---|---|---|---|---|---|---|
| **Zn** | 0 | 617.8 | 1.053 | 0.80 | 85.7 | 945 |
| | 24 | 443.2 | 3.021 | 0.65 | 347.5 | 1261 |
| | 48 | 414.6 | 3.976 | 0.56 | 588.6 | 1844 |
| **Zn−$CeO_2$** | 0 | 652.5 | 0.951 | 0.81 | 102.7 | 2764 |
| | 24 | 316.7 | 3.857 | 0.67 | 609.4 | 2214 |
| | 48 | 495.1 | 2.708 | 0.68 | 357.7 | 2195 |
| **Zn−$TiO_2 \cdot CeO_2$** | 0 | 732.5 | 0.851 | 0.78 | 67.8 | 1143 |
| | 24 | 577.6 | 3.416 | 0.67 | 391.8 | 1303 |
| | 48 | 464.5 | 4.376 | 0.61 | 361.7 | 1338 |

### 7.4.1.4. Salt spray tests

Neutral salt spray test according to SR EN ISO 9227 was carried out in order to check if the developed coatings meet the industrial requirements. Figure 7.13 shows the salt spray test results and in Fig. 7.14 (PhD Thesis) are depicted the microscopic images of the surfaces, in agreement with the evolution of the corrosion process in time.

The Zn and Zn−$TiO_2$ coatings show pitting corrosion (red rust) after less than 100 h, while Zn−$CeO_2 \cdot TiO_2$ and Zn−($CeO_2$+$TiO_2$) were more resistant. The test provides an additional support and confirms the enhancement of corrosion resistance property of zinc in simultaneous presence of $TiO_2$ and $CeO_2$ in the coating. These results are promising, however the application of conversion coatings after electrodeposition of Zn composite layer in order to improve their corrosion resistance should be considered.

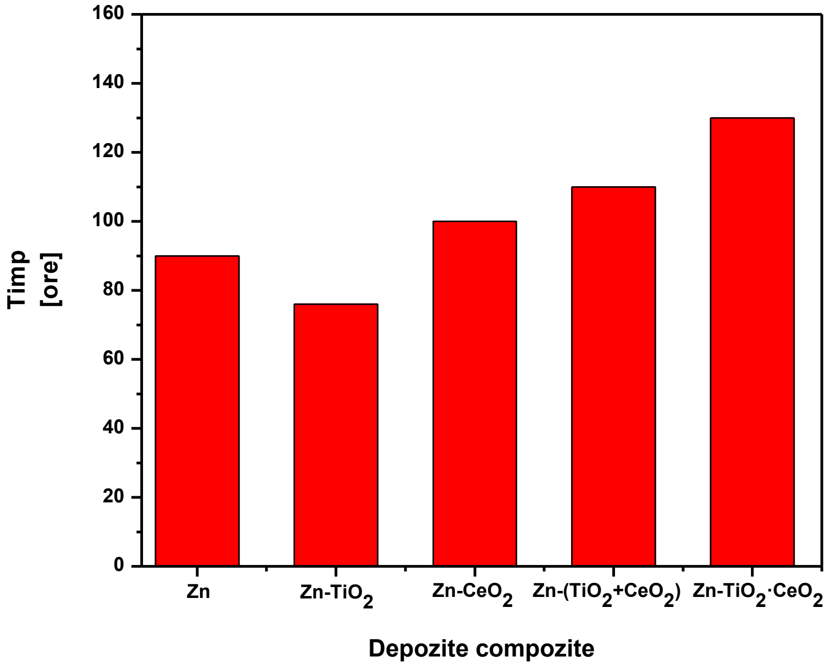

***Fig 7.13***. *Salt spray tests for the analyzed deposits*

## 7.5 Concluzii:

The analysis of the results led to the following conclusions:

- Even if the results are not spectacular, all the electrochemical measurements showed that the corrosion process on Zn−nanoparticles composite surface is slower than on pure zinc surface.
- The smallest value of the corrosion current density is noticed for Zn−$CeO_2$ deposit, followed by Zn−($CeO_2$+$TiO_2$) and Zn−$CeO_2$·$TiO_2$. The existence of a –Ti–O–Ce– network in the case of binary oxides ensures a more uniform distribution of cerium on the deposit surface than in the case of $CeO_2$+$TiO_2$ mixture, and hence, an increased protection.
- The codeposition of nanoparticles leads to changes in the morphology and structure of the nanocomposite coatings as compared to pure Zn coatings which could contribute to the increase of their corrosion resistance.

## 8. Corrosion behaviour of composite coatings with nanoparticles of $CeO_2$•$ZrO_2$ binary oxides

### 8.1 Aspecte generale

Zirconia possesses high resistance to wear and corrosion, biocompatibility, heat resistance and presents good adhesion to metallic surfaces [4,135]. Chemical vapour deposition, electrophoretic deposition and sol–gel deposition by dip coating procedure are common routes to prepare $ZrO_2$ coatings for anti−corrosion purposes and for the improvement of mechanical properties of the substrates [135,136].

Despite the large number of works published in literature reporting the unique properties of $CeO_2$ and $ZrO_2$, very little has been published about a combination of both in the field of the pre−treatments. It was shown that bis−1,2−[triethoxysilylpropyl]−tetrasulfide silane films containing $CeO_2 \cdot ZrO_2$ nanoparticles deposited by dip−coating on galvanised steel substrates are very efficient anticorrosion coatings [133]. The presence of zirconium ions provided very good barrier properties, whereas the presence of cerium provided better corrosion inhibition ability [133]. However, to the best of our knowledge, there are no reports on the preparation of composite layers by simultaneous co−deposition of zinc with $CeO_2$ and $ZrO_2$ nanoparticles.

In this context, the aim of this work is to investigate the effect of $CeO_2$ and $ZrO_2$ nanoparticles, used as a mechanical mixture or as binary $CeO_2 \cdot ZrO_2$ oxides on the corrosion resistance of zinc coatings, after the electro−co−deposition of nanoparticles with zinc. The method combines the advantages of metal electroplating (such as low cost, versatility and an easy process control) with those of composite materials and allows obtaining advanced materials with tailor−made properties [65].

X-ray diffraction (XRD) and SEM−EDX methods were used to determine the structure, the surface morphology and the chemical composition of the deposits. Polarization measurements followed by Tafel interpretation of the polarization curves were carried out in order to characterize the corrosion behaviour of the coatings.

### 8.3 Results and discussion

#### 8.3.1.2 X-ray diffraction

The XRD spectra of the investigated specimens are depicted in Figure 8.3. The main diffraction line can be attributed to the preferential hexagonal orientation of the zinc crystallites on the (101) direction, mainly determined by the presence of surfactants in the plating bath. It has been suggested that a preferred orientation of the zinc crystallites to the

(101) direction may facilitate a good co−deposition of ceria [1], and possibly of other nanoparticles as well.

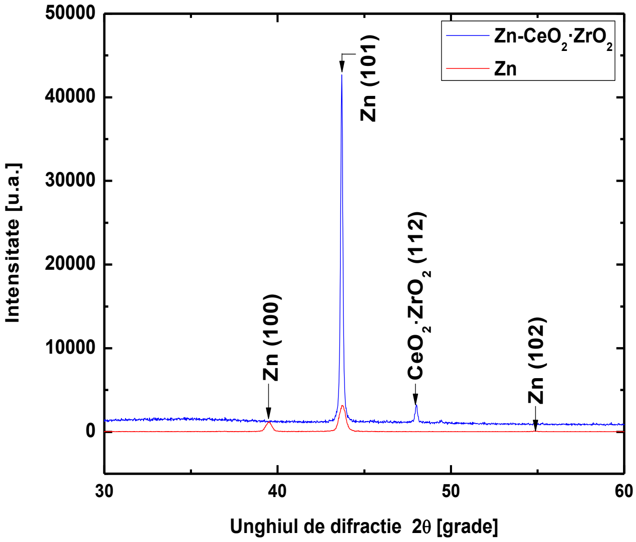

***Fig. 8.3.*** *XRD spectra for the Zn and Zn-*$CeO_2 \cdot ZrO_2$ *deposits*

Upon addition of the $CeO_2 \cdot ZrO_2$ oxide nanoparticles in the electrolytic bath, the diffraction lines of the resulting deposits exhibit a change in intensity, indicating a textural modification of the coating. The line corresponding to the (101) direction becomes more intense, while the (100) and (102) peaks decrease in height. At the same time, a new peak appears, corresponding to the (112) orientation, that can be attributed to the presence of $CeO_2 \cdot ZrO_2$ [142].

### 8.3.2.1 Open circuit potential

As it can be observed from Table 8.1, the open circuit potential values of the investigated samples recorded after one hour of immersion in the corrosive medium are relatively close to each other, with a variation of ±30 mV. The shifts towards a more negative potential in the presence of nanoparticles in the Zn deposit suggest the existence of an influence exerted by these particles on the oxygen reduction process.

The corrosion solution used for the electrochemical tests was $Na_2SO_4$, 0.2 g/L, pH=5.

***Tabel 8.1*** *Open circuit potential values for the obtained Zn and Zn−composite deposits*

| **Deposit** | **Nanoparticle concentration [g $L^{-1}$]** | **OCP [mV *vs* Ag/AgCl]** |
|---|---|---|
| **Zn** | 0 | −983 |
| **Zn−$ZrO_2$** | 1.25 | −1014 |
| **Zn−$CeO_2$** |  | −1011 |
| **Zn−$CeO_2$·$ZrO_2$** | 1.25 | −996 |
|  | 5 | −1008 |
| **Zn−$CeO_2$+$ZrO_2$** | 1.25 | −984 |
|  | 5 | −994 |

### 8.3.2.2 Potentiodynamic measurements

The results of OCP analysis were further endorsed by conducting polarization studies. The cathodic and anodic polarization curves of Zn, Zn−($CeO_2$·$ZrO_2$), Zn−($CeO_2$+$ZrO_2$), Zn−$ZrO_2$ and Zn−$CeO_2$ coatings recorded after 1h of immersion in $Na_2SO_4$ solution (pH 5) are presented in Figure 8.4 and 8.5. From the polarization curves, the corrosion parameters were evaluated by using only the anodic Tafel slopes, due to the fact that the cathodic branches of the polarization curves are flat (the cathodic process is controlled by the diffusion of $O_2$, being impossible to calculate $ß_c$). Thus, some degree of imprecision must be associated with the estimated corrosion rate under these conditions. However, a comparison between the behaviours of different deposits could be made, at least semi−quantitatively.

It has been established that a very low concentration of nanoparticles could be insufficient to enhance the corrosion resistance of the deposit, due to a too low percentage of nanoparticles embedded in the metallic matrix, while a too high concentration could generate defects in the coating, which can be starting points for generalized corrosion. Thus, an optimal concentration is required to be found for every particular system.

.

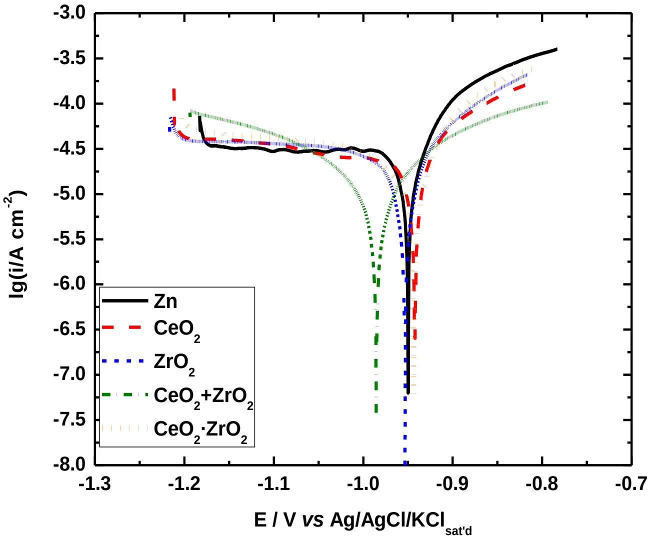

***Figure. 8.4.*** *Polarization curves (±200 mV vs OCP) for Zn and composite zinc deposits with a 1.25 g L$^{-1}$ concentration of nanoparticles*

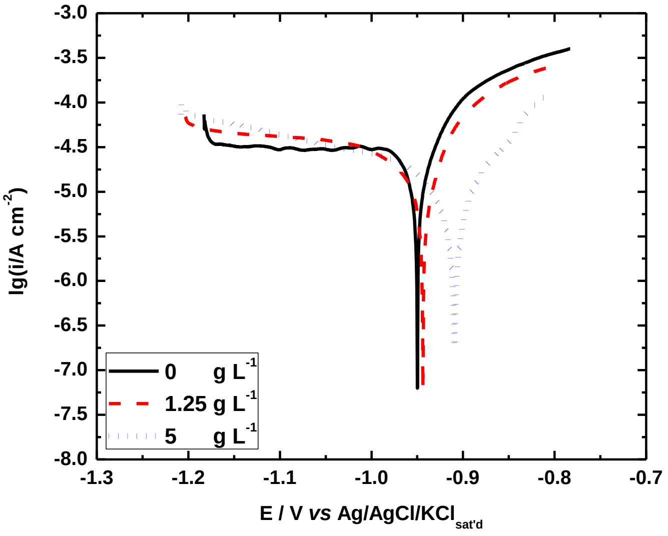

***Figure 8.5*** *Polarization curves (±200 mV vs OCP) for Zn and Zn−$CeO_2$·$ZrO_2$ deposits with various concentrations of nanoparticles*

The kinetic parameters for the corrosion process were estimated and are presented in Table 8.2.

The influence of the nanoparticles concentration on the corrosion behaviour of the composite coatings was already reported [56]. As it can be observed from Table 8.2, the lowest corrosion current density and the highest polarization resistance are noticed in the case when 5 g L$^{-1}$ binary $CeO_2$·$ZrO_2$ oxide nanoparticles were used.

In the case of the $CeO_2$+$ZrO_2$ mixture, the best corrosion resistance corresponded to 1.25 g $L^{-1}$concentration, closely followed by the 5 g $L^{-1}$ concentration. At the same time, it should be mentioned that in this case, the cathodic branches of the polarization curves recorded when the mixture is used, becomes mostly controlled by the charge transfer step, instead of the $O_2$ diffusion step.

At a concentration of 1.25 g $L^{-1}$ the most beneficial effect was noticed in the case of $CeO_2$+$ZrO_2$ mixture, followed by $ZrO_2$ and the binary $CeO_2$·$ZrO_2$ oxide, confirming the importance of the nature and properties of nanoparticles (size, surface charge, shape, previous treatments etc.) in the corrosion behavior of the composite deposits in which the nanoparticles are incorporated [143]. At the same time, by comparing the results obtained when $CeO_2$ and $ZrO_2$ were used separately, with those obtained in the presence of their mixture, it can be observed that a synergistic effect occurs when both are present, suggesting that the zirconia nanoparticles in combination with ceria offers a better protection than each type of nanoparticles used alone, both having a complementary role in this process.

***Table 8.2*** *Corrosion parameters estimated from potentiodynamic measurements for pure zinc deposit and for Zn−oxide nanoparticles composite coatings*

| **Deposit** | **Nanoparticle concentration [g $L^{-1}$]** | **$i_{corr}$ [μA $cm^2$]** | **$E_{corr}$ [mV *vs* Ag/AgCl]** | **$R_p$ [Ω $cm^2$]** | **$R^2$/N*** |
|---|---|---|---|---|---|
| **Zn** | 0 | 65.76 | −948 | 1272 | 0.99/17 |
| **Zn−$ZrO_2$** | 1.25 | 27.03 | −956 | 2679 | 0.99/25 |
| **Zn−$CeO_2$** | | 37.65 | −942 | 1767 | 0.99/22 |
| **Zn−$CeO_2$·$ZrO_2$** | 1.25 | 35.94 | −944 | 2027 | 0.99/25 |
| | 5 | 10.60 | −909 | 4542 | 0.99/27 |
| **Zn−$CeO_2$+$ZrO_2$** | 1.25 | 15.40 | −984 | 4063 | 0.99/23 |
| | 5 | 15.94 | −953 | 3420 | 0.99/42 |

## 8.4 Conclusions

The analysis of the results led to the following conclusions:

- The co−deposition of oxide nanoparticles with zinc leads to changes in the morphology of the resulting nanocomposite coatings as compared to pure Zn coatings. The composite coatings incorporating binary $CeO_2 \cdot ZrO_2$ oxides exhibited the highest corrosion resistance, due to the inclusion of the binary oxide in the metallic matrix.
- The physical and electrochemical properties of Zn coatings were best when the binary $CeO_2 \cdot ZrO_2$ and $CeO_2+ZrO_2$ mixture oxide nanoparticles were used. $CeO_2$ provides enhanced corrosion protection, with an effect on the oxygen reduction reaction, while $ZrO_2$ inhibits the corrosion process, and improves the wear resistance.
- The binary oxides used in optimal concentration (5 g $L^{-1}$) were proven to be more efficient than the simple mixture of the two oxides ($CeO_2$ and $ZrO_2$) probably due to the uniform distribution of Ce and Zr oxides on the surface of the composite samples (50:50 w:w).
- A synergistic effect was put in evidence when the two oxides were used in mixture as compared to individual ones.
- The corrosion properties of the composite coatings depend on the nanoparticles' concentration in the plating bath. Thus, an optimal concentration was put on evidence for the investigated nanocomposite deposits. The existence of an optimal concentration of nanoparticles is the result of the action of two contrary effects: on one hand, the nanoparticles have a beneficial influence, by reducing the active surface in contact with the corrosive medium and on the other hand, at a concentration that may be too high, they could generate defects in the metallic coating, stimulating corrosion.

## 9. GENERAL CONCLUSIONS

1. Several types of Zn composite coatings have been obtained on a steel substrate, by using two methods of eletrolytic codeposition, both in direct and in pulsed current. The electrolyte that was used was a mildly acidic chloride-based zinc plating bath, with and without additives, with different types and concentrations of nanoparticles.

2. The incorporation of nanoparticles in the metallic matric was demonstrated with EDX, XRD and GDOES.

3. According to the electrochemical measurements and the morpho-structural characterizations, it can be concluded that:

- the nanoparticles modify the morphology and structure of the deposits by influencing the competion between the nucleation process and the crystal growth process. Their presence tends to hinder the nucleation sites and determines the formation of new ones, thus obtaining more compact deposits.
- with more compact metallic depoists, the corrosion resistance is higher and the microhardness is increased.
- by embedding the nanoparticles, the surface roughness is smaller, and a decrease of the crystallite size has been noticed.

4. The modification of the current regime from a direct current to a pulsed current regime led to morphological and structural modifications, the Zn-nanoparticle layers having an increased compacity, a more clearer prefferential orientation, and of course, a higher corrosion resistance. Also, the use of pulsed current regime led to a more uniform distribution of nanoparticles within the deposit.

5. The concentration of the nanoparticles in the plating bath has an influence on the obtained composite deposits. From all the concentrations used, the best concentrations have been found, in agreement with the working conditions, for each composite system subjected to study,so that the best corrosion resistance of each deposit can be determined. The exitance of an optimal value for the concentration of the nanoparticles is the result of two contrary effects: on one hand, the nanoparticles have a good influence on the system, reducing the active surface in contact with the corrosive solution, on the other hand, if the concentration is

too high, the nanoparticles could generate defects in the metallic matrix, increasing the corrosion rates.

6. The stirring regime of the electrolyte is relevant to obtain quality deposits. The agglomeration phenomena in the zinc plating bath can be minimized by stirring the solution with high-power ultrasounds, which destroy the formed nanoparticle aggregates.
7. The nanocomposite system Zn-binary oxides has been studied for the first time, with the $TiO_2 \cdot CeO_2$ and $ZrO_2 \cdot CeO_2$ oxides, the first being sinthesized in the „Ilie Murgulescu" Physical Chemistry Institute laboratories, the latter being available commercially.
8. Comparisons between composite coatings with binary oxides and mechanical mixtures of the simple oxides that are used in the binary oxides have been made. It has been determined that the corrosion current density is lower in the case of the mechanical mixture of simple oxides, also, indicating that the presence of binary oxides in the metallic matrix offers a better corrosion protection than the pure zinc coating.
9. Lab-scale and pilot-scale experiments have been completed. It has been concluded that the experimental parameters that lead to the best results are different in the two cases, mainly because of the geometry of the cells. Thus, it was necessary to use a larger amount of $CeO_2$ nanoparticles in the plating bath in the pilot scale experiment (20 g/L vs 5 g/L used in the lab-scale experiments) in order to obtain a relatively constant concentration, on the surface and in the depth of the coating as well.

## 11. SELECTIVE REFERENCES

[1] Ranganatha, S., Venkatesha, T. V., Vathsala, K., & Kumar, M. K. P. (2012). Electrochemical studies on Zn/nano-$CeO_2$ electrodeposited composite coatings. *Surface and Coatings Technology*, *208,* 64–72. doi:10.1016/j.surfcoat.2012.08.004

[2] Nemeş, P. I., Zaharescu, M., & Muresan, L. M. (2013). Initial corrosion behavior of composite coatings obtained by co-electrodeposition of zinc with nanoparticles of Ti and Ce oxides, *17*(2), 511–518. doi:10.1007/s10008-012-1901-6

[3] Yen, S. K., Guo, M. J., & Zan, H. Z. (2001). Characterization of electrolytic $ZrO_2$ coating on Co-Cr-Mo implant alloys of hip prosthesis. *Biomaterials*, *22*(2), 125–33. Retrieved from http://www.ncbi.nlm.nih.gov/pubmed/11101157

[4] Devadasan, J. J., Sanjeeviraja, C., & Jayachandran, M. (2001). Electrodeposition of p-$WS_2$ thin film and characterisation. *Journal of Crystal Growth*, *226*, 67–72.

[5] Shi, L., Sun, C., & Liu, W. (2008). Electrodeposited nickel–cobalt composite coating containing MoS2. *Applied Surface Science*, *254*(21), 6880–6885. doi:10.1016/j.apsusc.2008.04.089

[6] Hou F Wang W Guo H (2006) Appl Surf Sci 252:3812–3817

[7] Xue, Y.-J., Jia, X.-Z., Zhou, Y.-W., Ma, W., & Li, J.-S. (2006). Tribological performance of Ni–$CeO_2$ composite coatings by electrodeposition. *Surface and Coatings Technology*, *200*(20-21), 5677–5681. doi:10.1016/j.surfcoat.2005.08.002

[8] Saber, K., Koch, C. ., & Fedkiw, P. . (2003). Pulse current electrodeposition of nanocrystalline zinc. *Materials Science and Engineering: A*, *341*(1-2), 174–181. doi:10.1016/S0921-5093(02)00198-3

[9] Kh. M. S. Youssef, C. C. Koch, P. S. Fedkiw - Improved corrosion behavior of nanocrystalline zinc produced by pulse-current electrodeposition, Corrosion Science, 46, (2004), 51. 33.

[10] Frade, T., Bouzon, V., Gomes, a., & da Silva Pereira, M. I. (2010). Pulsed-reverse current electrodeposition of Zn and Zn-$TiO_2$ nanocomposite films. *Surface and Coatings Technology*, *204*(21-22), 3592–3598. doi:10.1016/j.surfcoat.2010.04.030

[25] Szczygieł, B., & Kołodziej, M. (2005). Composite Ni/$Al_2O_3$ coatings and their corrosion resistance. *Electrochimica Acta*, *50*(20), 4188–4195. doi:10.1016/j.electacta.2005.01.040

[56] Low, C. T. J., Wills, R. G. a., & Walsh, F. C. (2006). Electrodeposition of composite coatings containing nanoparticles in a metal deposit. *Surface and Coatings Technology*, *201*(1-2), 371–383. doi:10.1016/j.surfcoat.2005.11.123

[61] Y. Suzuki, O. Asai, J. Electrochem. Soc, 134 (1987), 1905

[66] Fransaer, J. (1992). Analysis of the Electrolytic Codeposition of Non-Brownian Particles with Metals. *Journal of The Electrochemical Society*, *139*(2), 413. doi:10.1149/1.2069233

[70] F. Fontenay, L. B. Andersen, P. Moller, *Electroplating and characterization of zinc composite coatings*, Galvanotechnik, 2001, 92 (4) pp:928

[98] Ivanov, V. K., Usatenko, a. V., & Shcherbakov, a. B. (2009). Antioxidant activity of nanocrystalline ceria to anthocyanins. *Russian Journal of Inorganic Chemistry*, *54*(10), 1522–1527.

[99] Cao, X. Q., Vassen, R., & Stoever, D. (2004). Ceramic materials for thermal barrier coatings. *Journal of the European Ceramic Society*, *24*(1), 1–10.

[100] Hamlaoui Y Pedraza F Tifouti L (2008) Corros Sci 50:2182–2188

[101] Davó, B., & de Damborenea, J. J. (2004). Use of rare earth salts as electrochemical corrosion inhibitors for an Al–Li–Cu (8090) alloy in 3.56% NaCl. *Electrochimica Acta*, *49*(27), 4957–4965.

[102] Davó, B., Conde, a., & de Damborenea, J. J. (2005). Inhibition of stress corrosion cracking of alloy AA8090 T-8171 by addition of rare earth salts. *Corrosion Science*, *47*(5), 1227–1237.

[103] Bethencourt, M., Botana, F. J., Calvino, J. J., Marcos, M., & RodrÍguez-Chacón, M. a. (1998). Lanthanide compounds as environmentally-friendly corrosion inhibitors of aluminium alloys: a review. *Corrosion Science*, *40*(11), 1803–1819.

[104] Shibli, S. M. a., & Chacko, F. (2008). Development of nano $CeO_2$-incorporated high performance hot-dip zinc coating. *Surface and Coatings Technology*, *202*(20), 4971–4975. doi:10.1016/j.surfcoat.2008.04.090

*of Rare Earths*, *26*(4), 579–583.

[111] Punith Kumar, M. K., Venkatesha, T. V, Pavithra, M. K., & Nithyananda Shetty, a. (2011). The fabrication, characterization and electrochemical corrosion behavior of Zn-$TiO_2$ composite coatings. *Physica Scripta*, *84*(3), 035601.

[112] Xia, X., Zhitomirsky, I., & McDermid, J. R. (2009). Electrodeposition of zinc and composite zinc–yttria stabilized zirconia coatings. *Journal of Materials Processing Technology*, *209*(5), 2632–2640.

[113] Youssef, K. M., Koch, C. C., & Fedkiw, P. S. (2008). Influence of pulse plating parameters on the synthesis and preferred orientation of nanocrystalline zinc from zinc sulfate electrolytes. *Electrochimica Acta*, *54*(2), 677–683.

[115] Xuetao, Y., Yu, W., Dongbai, S., & Hongying, Y. (2008). Influence of pulse parameters on the microstructure and microhardness of nickel electrodeposits. *Surface and Coatings Technology*, *202*(9), 1895–1903.

[118] Wang, Y., Kovacevic, R., & Liu, J. (1998). Mechanism of surface modification of $CeO_2$ in laser remelted alloy spray coatings. *Wear*, *221*, 47–53.

[119] Schem, M., Schmidt, T., Gerwann, J., Wittmar, M., Veith, M., Thompson, G. E., … Zheludkevich, M. L. (2009). $CeO_2$-filled sol–gel coatings for corrosion protection of AA2024-T3 aluminium alloy. *Corrosion Science*, *51*(10), 2304–2315.

[120] Shibli, S. M. a., Archana, S. R., & Muhamed Ashraf, P. (2008). Development of nano cerium oxide incorporated aluminium alloy sacrificial anode for marine applications. *Corrosion Science*, *50*(8), 2232–2238.

[121] Yu YC, Yves MB (1993) Corrosion Science 34:1773−1781

[122] Hamlaoui, Y., Rémazeilles, C., Bordes, M., Tifouti, L., & Pedraza, F. (2010). Electrodeposition of ceria-based layers on zinc electroplated steel. *Corrosion Science*, *52*(3), 1020–1025. doi:10.1016/j.corsci.2009.11.027

[123] Hamlaoui, Y., Pedraza, F., Remazeilles, C., Cohendoz, S., Rébéré, C., Tifouti, L., & Creus, J. (2009). Cathodic electrodeposition of cerium-based oxides on carbon steel from concentrated cerium nitrate solutions. *Materials Chemistry and Physics*, *113*(2-3), 650–657. doi:10.1016/j.matchemphys.2008.08.027

[124] Gomes, a., Pereira, M. I., Mendonça, M. H., & Costa, F. M. (2004). Zn–$TiO_2$ composite films prepared by pulsed electrodeposition. *Journal of Solid State Electrochemistry*, *9*(4), 190–196. doi:10.1007/s10008-004-0573-2

[125] Wang, S.-C., & Wei, W.-C. J. (2003). Kinetics of electroplating process of nano-sized ceramic particle/Ni composite. *Materials Chemistry and Physics*, *78*(3), 574–580. doi:10.1016/S0254-0584(01)00564-8

[126] Celis, J. P. (1987). A Mathematical Model for the Electrolytic Codeposition of Particles with a Metallic Matrix. *Journal of The Electrochemical Society*, *134*(6), 1402. doi:10.1149/1.2100680

[127] Maurin, G., Lavanant, A. (1995). Electrodeposition of nickel/silicon carbide composite coatings on a rotating disc electrode. *Journal of Applied Electrochemistry*, *25*, 1113–1121.

[128] Hwang, B. J., Hwang, C. S. (1993). Mechanism of Codeposition of Silicon Carbide with Electrolytic Cobalt. *Journal of The Electrochemical Society*, *140*(4), 979. doi:10.1149/1.2056239

[129] Shao, I., Vereecken, P. M., Cammarata, R. C., & Searson, P. C. (2002). Kinetics of Particle Codeposition of Nanocomposites. *Journal of The Electrochemical Society*, *149*(11), C610. doi:10.1149/1.1514672

[130] Pagetti, J., Bercot, P., & Peña Muñoz, E. (2002). Electrolytic composite Ni – PTFE coatings : an adaptation of Guglielmi ’ s model for the phenomena of incorporation, *157*, 282–289.

[133] Montemor, M. F., Trabelsi, W., Lamaka, S. V., Yasakau, K. a., Zheludkevich, M. L., Bastos, a. C., & Ferreira, M. G. S. (2008). The synergistic combination of bis-silane and $CeO_2 \cdot ZrO_2$ nanoparticles on the electrochemical behaviour of galvanised steel in NaCl solutions. *Electrochimica Acta*, *53*(20), 5913–5922. doi:10.1016/j.electacta.2008.03.069

[134] Juettner K, Lorenz WJ, Kendig MW, Mansfeld F (1988) J Electrochem Society 135:332

[135] Sui, J. H., & Cai, W. (2006). Formation of $ZrO_2$ coating on the NiTi alloys for improving their surface properties. *Nuclear Instruments and Methods in Physics Research Section B: Beam Interactions with Materials and Atoms*, *251*(2), 402–406. doi:10.1016/j.nimb.2006.06.028

[136] Fu, Y.-P., Hu, S.-H., & Liu, B.-L. (2009). Structure characterization and mechanical properties of $CeO_2$–$ZrO_2$ solid solution system. *Ceramics International*, *35*(8), 3005–3011. doi:10.1016/j.ceramint.2009.04.001

[142] Zhang, F., Chen, C., Raitano, J. M., & Hanson, J. C. (2006). Phase stability in ceria-zirconia binary oxide nanoparticles : The effect of the $Ce^{3+}$ concentration and the redox environment. *Journal Of Applied Physics*, *99*(May), 1–8. doi:10.1063/1.2190712

[143] Zanella, C., Lekka, M., & Bonora, P. L. (2008). Influence of the particle size on the mechanical and electrochemical behaviour of micro- and nano-nickel matrix composite coatings. *Journal of Applied Electrochemistry*, *39*(1),31–38.

## 12. PUBLICATIONS AND SCIENTIFIC PROCEEDINGS LIST

### Articles

1. P. Nemeş, M. Zaharescu, L. M. Mureşan, *Journal of Solid State Electrochemistry*, **2013**, 17, (2), 511-518, I.F. ISI 2012: 2.279

2. P. Nemeș, N. Coțolan, L. M. Mureșan, *Studia Universitatis Babeș Bolyai, Chemia,* **2013**, LVIII, (1), 81-91.

3. P. Nemeș, M. Lekka, L. Fedrizzi, L.M.Mureșan, *Influence of the electrodeposition current regime on the corrosion resistance of Zn-*$CeO_2$ nanocomposite coatings; sent to Hydrometallurgy – Decembrie 2013.

### Published in volumes:

1. Patrick Ioan Nemes, L.M. Muresan, M. Zaharescu, Electrochemical properties of electrodeposited composite zinc-nanoparticles coatings on steel, *Proc. of the International Conference "Environmental Engineering and Sustainable development",* Alba-Iulia, **2011**, p. 341-346, ISBN 978-606-613-002-8

### Scientific communications:

1. Nemes Patrick Ioan, Liana Maria Muresan, Maria Zaharescu, Electrochemical properties of electrodeposited composite zinc – nanoparticles coatings on steel, INTERNATIONAL U.A.B. – B.EN.A. CONFERENCE. ENVIRONMENTAL ENGINEERING AND SUSTAINABLE DEVELOPMENT, Alba Iulia, Romania, 26-27 Mai, 2011

2. Nemeș Patrick, Liana Muresan, Maria Zaharescu, Electrochemical and morphostructural characterization of Zn- nanoparticles composite deposits obtained by electrodeposition, A VI-a Conferinta Nationala cu participare Internationala de Coroziune si Protectie Anticoroziva, Cluj Napoca, 22-24 septembrie 2011.

3. Nemeș Patrick Ioan, Liana Maria Mureșan, Maria Zaharescu, Nanocomposite Coatings obtained by electrolytic codeposition of zinc with nanoparticles of binary $TiO_2 \cdot CeO_2$ oxides, RSE-SEE3 (Regional Symposium on Electrochemistry), București, ROMANIA, 13-17 Mai, 2012 – POSTER.

4. Nemes Patrick Ioan, Maria Lekka, Lorenzo Fedrizzi, Liana M. Muresan, Influence of the electrodeposition current regime on the corrosion resistance of Zn-$CeO_2$ nanocomposite coatings, Fourth Regional Symposium on Electrochemistry South East Europe (RSE-SEE 4), Ljubliana, Slovenia, 26-30 Mai, 2013.